Phase Transitions

DOI: 10.1002/anie.201200407

Bis(imidazolium) L-Tartrate: A Hydrogen-Bonded Displacive-Type Molecular Ferroelectric Material**

Zhihua Sun, Tianliang Chen, Junhua Luo, and Maochun Hong*

Ferroelectric materials have attracted great attention both in condensed-matter science and as materials for versatile technical applications, such as ferroelectric random-access memories, ferroelectric field-effect transistors, and infrared detectors.[1] Since Rochelle salt (potassium sodium tartrate tetrahydrate) was first discovered as ferroelectric material,[2a] numerous ferroelectric compounds have been investigated, including inorganic perovskite oxides,[2b,c] organic–inorganic hybrids,[2d–g] and organic ferroelectric materials.[2h,i] Among the latter ones, hydrogen bonds in ionic and organic complexes can be considered as donor–acceptor systems (H atom is acceptor, whereas N, O, or halogen atoms are donors). H-bonds are directional but weaker than covalent bonds when binding atoms in molecules. Thus, aggregates constructed by H-bonds easily undergo transformations that are induced by the cleavage and formation of other H-bonds, by proton transfers, or by disordering. Such transformations change the properties and/or functions of materials; for example, O–H···O H-bonds in KH_2PO_4 (KDP) crystals are well-known to undergo a ferroelectric phase transition.[3] However, exploration of novel ferroelectric materials that contain H-bonds still remains a challenge,[4] because the ferroelectric materials should meet several requirements, such as having a phase transition, a good electric hysteresis loop, a dielectric anomaly or electric domain motion, and the necessary crystallographic requirements of one of the ten polar point groups in the ferroelectric phase (C_1, C_2, C_s, C_{2v}, C_4, C_{4v}, C_3, C_{3v}, C_6, and C_{6v}).

Rochelle salt derivatives appeared to be thoroughly exploited as ferroelectric materials with regard to their physical properties; proton dynamics of the hydroxy group of L-tartrate together with atomic displacements cause ferroelectricity during the phase transition.[5] However, rare novel ferroelectric compounds were discovered in this family.[4a,5d] Ferroelectricity in compounds with different organic components has been observed after displacing the oppositely charged counterions to give H-bonded complexes,[6] and the dimerization of electron donor and acceptor causes phase transition or dielectric abnormity. Simple organic molecular rotators, such as imidazole, have been utilized to develop artificial molecular motors or potential dielectric rotors;[7] that is, molecular rotator units have been used to obtain new ferroelectric materials. Herein, we introduce a new organic H-bonded molecular ferroelectric material, bis(imidazolium) L-tartrate (complex **1**), with imidazole as a classical molecular rotator and L-tartaric acid as homochiral component, which provides potential hydrogen donor/acceptor functionalities and guarantees the possible crystallization in the polar point group. To the best of our knowledge, **1** undergoes a paraelectric–ferroelectric phase transition at 252 K with an exceptional dielectric response and a good spontaneous polarization triggered by the atomic displacements, thus, **1** was disclosed as a novel organic ferroelectric compound assembled by a homochiral ligand with an organic molecular rotator.

Complex **1** was prepared by slow evaporation of an aqueous solution of imidazole and L-tartaric acid in a molar ratio of 2:1. Bulk high-quality colorless crystals with perfect morphology ($25 \times 14 \times 8\ mm^3$) were obtained by the temperature-lowering method after several days (Figure S1). The straightforward fabrication of high-quality crystals with large size guarantees their potential application in devices. The phase purity of the crystals was confirmed by matching the signal pattern of X-ray powder diffraction (XRPD) analysis at room temperature with the calculated pattern (Figure S2). Differential scanning calorimetry (DSC) clearly showed a solid–solid phase transition of **1** at approximately 252 K in the heating mode (Figure S3), which is also confirmed by the reversible endothermic anomaly. The entropy change ΔS that accompanied the transition was estimated to be approximately $3.9\ J\,mol^{-1}\,K^{-1}$. With the Boltzmann equation $\Delta S = R \ln N$, in which R is the gas constant and N is the ratio of the numbers of respective geometrically distinguishable orientations, $N = 1.6$ is obtained. This N value, which is smaller than two, indicates a complicated phase transition. The phase-transition temperature (T_c) of the deuterated complex was 5 K higher than that of nondeuterated complex **1** in both the heating and cooling modes, and the shape of the anomaly was similar; that is, substituting hydrogen by deuterium leads to an increase of the T_c.[2e] In contrast, the racemic tartrate does not assemble with imidazole to the analogous ferroelectric complex. Only a fine white powder was obtained, and the inability to grow bulk crystals restricted the potential dielectric or even ferroelectric characterization of such

[*] Dr. Z. Sun, T. Chen, Prof. J. Luo, Prof. M. Hong
Key Laboratory of Optoelectronic Materials Chemistry and Physics
Fujian Institute of Research on the Structure of Matter
Chinese Academy of Sciences
Fuzhou, Fujian 350002 (P.R. China)
E-mail: jhluo@fjirsm.ac.cn

[**] This work was financially supported by the NSFC (grants 51102231 and 21171166), the One Hundred Talent Program of the Chinese Academy of Sciences, and the 973 Key Programs of the MOST (grants 2010CB933501 and 2011CB935904). We gratefully thank Prof. R.-G. Xiong and his co-workers for their help on the dielectric and ferroelectric measurements and valuable discussions, Prof. X.-Y. Chen for the variable-temperature second harmonic generation measurement, and the reviewers for their excellent suggestions.

Supporting information for this article is available on the WWW under http://dx.doi.org/10.1002/anie.201200407.

a material. Furthermore, neither DSC nor dielectric experiments on the powder sample of the racemic compound showed an obvious anomaly (Figure S4), meaning the absence of phase transition, which might be ascribed to the opposite stoichiometric effect of L and D components. The results confirm the effectiveness to assemble ferroelectric materials with the homochiral ligand as the building block.

Variable-temperature single-crystal X-ray diffraction indicates that the asymmetric unit of the solid-state structure of **1** at room temperature (293 K, RT) is composed of one L-tartrate anion and two imidazolium cations, while in the low-temperature phase (93 K, LT) the asymmetric unit is doubled with a slightly distinctive structure (Figure 1 and S5).[8] Here, the pseudosymmetry analysis is used, in which a given low-symmetry (ferroelectric) structure is represented in terms of a symmetry-lowering Landau-type structural phase transition from a high-symmetry (paraelectric) parent structure, based on finding a supergroup of the given space group. The crystal structure of **1** at RT classifies as an orthorhombic crystal system with the space group $P2_12_12_1$ and a nonpolar point group D_2, and exhibits paraelectric features (Table S1). The different structure at LT confirms that **1** changes to a lower symmetric state below T_c. When the temperature is decreased below 252 K, the crystal structure changes into a monoclinic crystal system with the space group $P2_1$ and a polar point group C_2, thus giving a ferroelectric phase (Figure 1). During the cooling process, symmetry occurs with an Aizu notation of $222F2$; namely, the four symmetric elements (E, C_2, C_2', C_2'') in the paraelectric phase are reduced to two (E, C_2) in the ferroelectric phase in accordance with the Landau phase-transition theory. According to the Curie symmetry principle, the space group in the LT phase ($P2_1$) is a subgroup of that in the high-temperature (HT) phase ($P2_12_12_1$), a result that is in perfect agreement with the symmetry-breaking analysis and the Landau theory. Structurally, all molecules are helically located around the center of rotation without any disorder in the atomic positions. Both RT and LT crystal structures are constructed by a three-dimensional H-bonds network with two types of H-bonds: 1) O–H···O H-bonds between L-tartrate anions form infinite spiral ribbons elongated along the RT *a*-axis, and 2) N–H···O H-bonds between L-tartrate anions and imidazolium cations, linking them together in the three-dimensional H-bonds network. Furthermore, according to the crystal packing views, a tiny distinction between RT and LT exists, owing to the participation of all N atoms of the central imidazolium cations, which are guests inside the channel, in H-bonds and thus forming bridges across the channel with N–H···O H-bonds (see Figure 1 and S6, Tables S5 and S9).

Measurements of the temperature dependence of the dielectric permittivity of **1** were carried out on single-crystal samples in the heating mode, under the applied electric field $E||a$-axis (RT) with frequencies of 1 kHz to 1 MHz (Figure 2). The real component shows very large maxima of dielectric anomaly around 252 K, corresponding to the phase transition. Indeed, the maximum ε' values vary slightly with the frequency, and are up to ten times higher than those at higher and lower temperatures, which is the characteristic feature for the phase transition. To verify the continuous

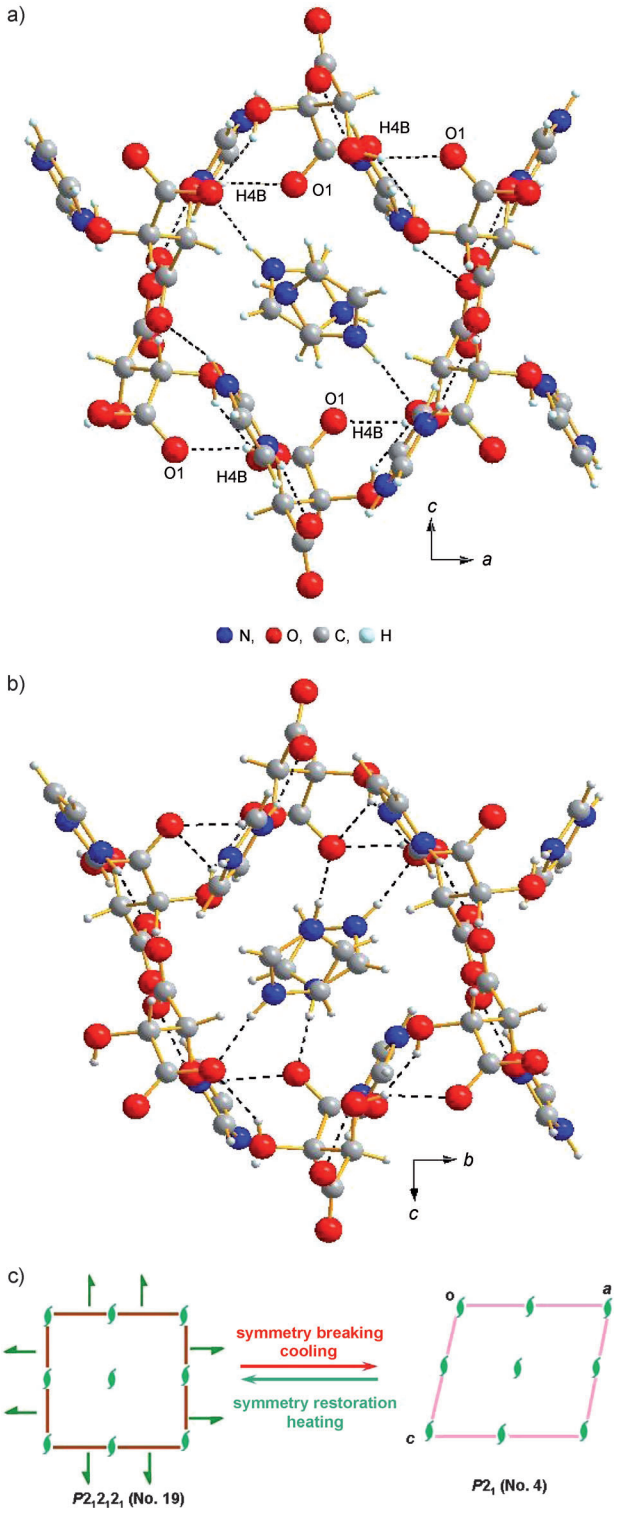

Figure 1. a) The packing diagram viewed along the *b*-axis in the paraelectric phase; b) the packing diagram viewed along the *a*-axis in the ferroelectric phase; H-bonds: black-dotted lines; c) transformation of the space group of **1** from paraelectric phase to ferroelectric phase.

properties of this phase transition, the temperature dependence of the reciprocal ε' value was plotted (see insert in Figure 2a); between 220 and 290 K the corresponding results at 10 kHz are in good agreement with the Curie–Weiss law $\varepsilon =$

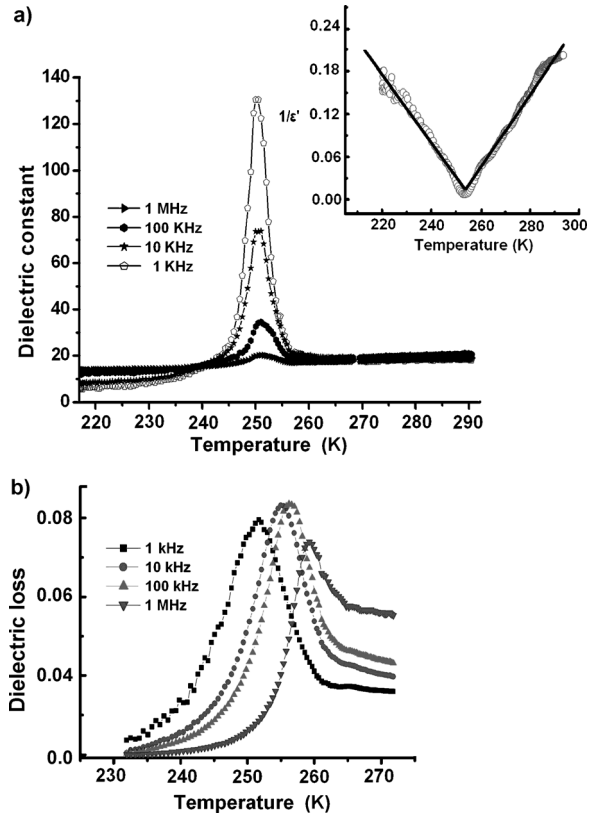

Figure 2. Temperature-dependence of the complex dielectric constant along the RT *a*-axis: a) Real part (ε′) at different frequencies. The inset shows the reciprocal of the real part of the complex dielectric constant versus the temperature; b) imaginary part (ε″) at different frequencies.

$\varepsilon_0 + C/(T-T_0)$, thus affording the Curie–Weiss temperature $T_0 = 250$ K and the Curie constant $C_{ferro} = 127$ K. The value of C_{ferro} from this linear $1/\varepsilon - T$ relationship is comparable to those of typical ferroelectric materials containing H-bonds, and the deduced T_0 is slightly lower than $T_c = 252$ K. The value of C_{para} of the paraelectric phase is 212 K, which is comparable with those found for ferroelectric compounds, such as NH_4HSO_4, $(NH_2CH_2COOH)_2HNO_3$, and $(CH_3NH_3)Al(SO_4)_2 \cdot 12H_2O$ with values of around 200 K.[9] Thus, the ratio of Curie–Weiss constants $C_{para}/C_{ferro} = 1.7$, which is smaller than 4.0, also suggests the complicated phase transition.[9]

Another feature of the dielectric properties of **1** is a "relaxor-like" relaxation process, which is more obvious for the imaginary part (ε″; Figure 2b), thus revealing that the dielectric loss changes with the temperature at different frequencies with the peak maxima obeying the Arrhenius equation $\tau = \tau_0 \exp(E_a/k_B T)$, in which T is the temperature, k_B denotes the Boltzmann constant, E_a denotes the activation energy, and τ_0 is the inverse of the frequency factor. For a Debye peak, the equation can be rewritten as $\ln f = -\ln(2\pi\tau_o) - E_a/k_B T_p$, considering the peak condition of $2\pi f\tau = 1$, in which f is the frequency. Hence, the activation energy E_a is estimated to be approximately 296 kJ mol^{-1}, which is similar to that of compounds reported by You et al.[10b] but larger than that of common dielectric processes (10–70 kJ mol^{-1}).[10] Such a process, which has been observed in several organic ferroelectric compounds, including Rochelle salt,[11] is probably associated with the dipolar reorientation or the proton transfer. In the case of our compound, the high E_a value may be ascribed to the hindrance to the dipole motion by the ferroelectric interactions between dipoles, which is also consistent with the structural analysis of the complicated H-bonding interaction.

Second harmonic generation (SHG) has been extensively used to confirm the ferroelectric domain structure and phase transition as a result of changing temperature, especially for the symmetry breaking from a centrosymmetric structure to a non-centrosymmetric one.[2j,12] According to the Landau theory, the second-order nonlinear optical (NLO) susceptibilities $\chi^{(2)}$ can be described as $\chi^{(2)} = 6\varepsilon_0 \beta P_s$ if higher-order items are ignored.[4c,12d] Considering that β is nearly independent of the temperature, the expression indicates that $\chi^{(2)}$ is proportional to the saturation polarization P_s. Here, the temperature-dependent SHG signal of **1** was recorded between 150 and 300 K (Figures 3 and S7). Complex **1**

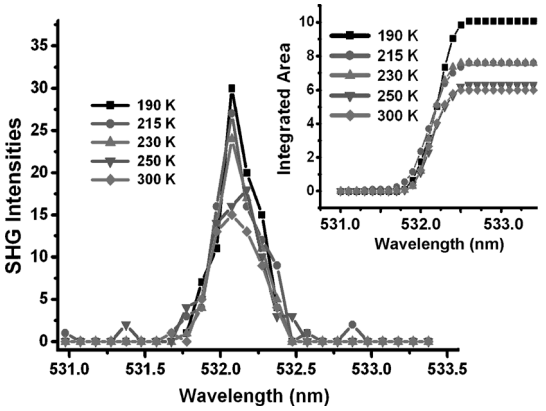

Figure 3. The variable-temperature experimental SHG signal of **1** at 532 nm. Inset: The integrated area of corresponding signal curves for the approximate comparison of signal intensities.

exhibits an obvious SHG signal around 532 nm in both paraelectric and ferroelectric phases, which is in fairly good agreement with the non-centrosymmetric structures. SHG intensities of **1** were estimated by comparison with those of KDP standard samples, and were about 2.5 times as large as that of KDP. That is, **1** may also be considered as a potential organic NLO material. Additionally, a slightly increasing tendency of SHG intensity is found in its ferroelectric phase, which is similar to several displacive-type ferroelectric materials, such as $LiTaO_3$, $LiNbO_3$, and CMAP (4-(cyanomethyl)anilinium perchlorate).[4c] These observations suggest that the primary contribution to the ferroelectricity of **1** might be of a displacive type.

The ferroelectric nature of **1** has been directly proven by hysteresis measurements of the electric polarization (P) versus electric field (E) at about 20 K below T_c. The P–E loop under the electric field of triangle waveform was recorded approximately along the *a*-axis (Figure 4a). Initially, a straight line is observed without any change down to 252 K,

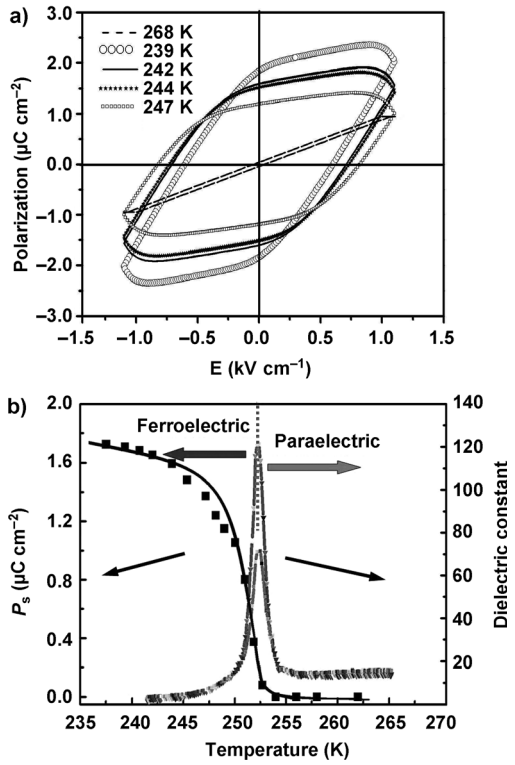

Figure 4. a) Dielectric hysteresis loops of **1** with E| |*a*-axis at various temperatures; b) Temperature dependence of the saturated polarization P_s.

thus showing the paraelectric feature. Then, the line opens and becomes a typical ferroelectric loop at around 247 K. Furthermore, the loop reaches its saturation at 235 K with the spontaneous polarization $P_s = 1.72\ \mu C\,cm^{-2}$, the remanent polarization $P_r = 1.56\ \mu C\,cm^{-2}$, and the corresponding electric field $E_c \approx 1.1\ kV\,cm^{-1}$. Coinciding with the phase transition, the P_s values are nearly stable around 235 K (Figure 4b), and the magnitude is consistent with those of typical ferroelectric materials containing H-bonds,[2h] but much larger than those of ferroelectric L-tartrate crystals, such as Rochelle salt (Table S10). Moreover, the dipole moment calculated from the saturated polarization derived from the *P*–*E* curve is $\mu_s = V_{cell} P_s/Z$ (1.35×10^{-30} Cm), with the density of *D*–*A* dipolar pairs estimated as $3.148 \times 10^{27}\ m^{-3}$ with four dipoles in the unit cell ($Z = 4$). The effective paraelectric moment derived from the $C = Z\mu_c^2/k_B\varepsilon_0 V_{cell}$ (k_B = Boltzmann constant; ε_0 = permittivity of vacuum) is $\mu_c = 2.22 \times 10^{-30}$ Cm. The ratio of μ_c/μ_s is approximately 1.63:1 and is thus rather close to those of several displacive-type ferroelectric materials, which are distinct from order-disorder type ferroelectric compounds having μ_c/μ_s ratios of approximately 1:1.[6b,13]

The results of dielectric and hysteresis-loop experiments clearly show the ferroelectricity of **1** in the LT phase. Taking into account the extensive research on ferroelectricity in the Rochelle salt family, this novel ferroelectric material is quite an unexpected discovery. However, clarifying the distinct origin of the ferroelectricity of **1** remains challenging, owing to the more complicated structure of **1** compared with Rochelle salt. Generally, it is disputably recognized that the proton dynamics in the hydroxy group of L-tartrate together with atomic displacements are contributing to the ferroelectricity of Rochelle salt.[4a,14] The current X-ray diffraction results of **1** may merely present no change in proton dynamics. Thus, it is necessary to perform the neutron diffraction analysis on **1** to determine the positions of the hydrogen atoms in the bridges, which will be a subject of forthcoming experiments. Currently, it may be deduced that the small change of crystal packing during phase transition might contribute to the appearance of polar properties in LT phase. The symmetric operations of twofold screw axes exist along three crystallographic directions with imidazolium cations lying perpendicularly to the RT *a*-axis. When the temperature decreases, the *bc* plane undertakes a slight shearing transformation, thus causing the symmetric operations of twofold screw in this plane to disappear; namely, the breaking of symmetry occurs. Thus, the LT *b*-axis was determined as the exclusive polar direction to minimize the change of its length and the obtuse monoclinic angle β, as is commonly recommended in the ferroelectric phase. The total macroscopic polarization is parallel to the LT *b*-axis, owing to *a* and *c* components being cancelled out. A comparison of the crystal structures of **1** in HT and LT phases allows us to deduce the possible origin for its spontaneous polarization below T_c (Tables S2 to S9). Little deformation of imidazole and L-tartrate molecules was observed during the phase transition. The important contribution to the spontaneous polarization of **1** arises from the representative displacement in the O···O separation (Figure 5). In the paraelectric phase, the O···O distances of two typical O–H···O H-bonds in the

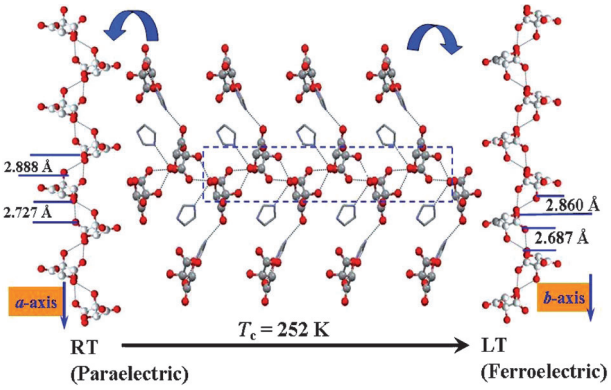

Figure 5. Schematic illustration of the representative O···O separations in the ribbon during the phase transition.

anion ribbons are 2.727 and 2.888 Å, respectively. However, in the LT phase, the corresponding values decrease to 2.687 and 2.860 Å, thus confirming the atomic displacement along the polar direction during the phase transition.[5c, 15] The above-mentioned result supports the theory that the phase transition is not order–disorder but displacive type, which is also consistent with the X-ray diffraction results and the conclusion drawn from the ratio of dipolar moments. When we assumed two point charges of cation and anion, the atomic displacement (δ) is estimated to be approximately $\delta = P_s V_{cell}/Zq = 0.08$ Å, in which q is ± 2 e.[15b] The experimental (0.04 Å)

and estimated (0.08 Å) difference might be accounted for the intermolecular interactions in this complicated ferroelectric system. Moreover, whether the switching of H-bonds parallel to the RT *a*-axis (O_1–H_{4B}···O_4) ascribes to the optimization of hydrogen in the hydroxy group of L-tartrate anions during the phase transition and accounts for the spontaneous polarization will be investigated by the forthcoming neutron diffraction experiments.

In conclusion, the present work has successfully demonstrated a novel H-bonded molecular ferroelectric material, bis(imidazolium) L-tartrate, by co-crystallization of the homochiral ligand with a molecular rotator, which undergoes the paraelectric–ferroelectric phase transition at 252 K with an exceptional dielectric response triggered with the atomic displacements. It possesses the promising large electric polarization, dielectric susceptibility, and small coercive field. We believe these results urge the exploration of new ferroelectric materials and polar functional materials.

Experimental Section

X-ray powder diffraction (XRPD) was measured on a MiniFlex II X-ray diffraction instrument. DSC experiments were performed on a NETZSCH DSC 200 F3 under nitrogen atmosphere in aluminum crucibles with the heating and cooling rate of 10 K min^{-1}. In the dielectric experiments, the polished single-crystal samples were covered by silver conduction paste on the surfaces as the electrodes. Complex dielectric permittivities were measured using a TH2828 A Impedance Analyzer with an applied electric field of 0.5 V. The overall error was less than 5% for the experimental results. The hysteresis loop was recorded with a simple Sawyer-Tower circuit at 100 Hz at different temperatures. X-ray single-crystal diffraction data were collected on a Rigaku Saturn70 diffractometer with Mo-Kα radiation ($\lambda = 0.71073$) with the variable temperatures. CrystalClear software package (Rigaku) was used for data collection, cell refinement and data reduction. The crystal structures were solved by direct methods and refined by the full-matrix method based on F^2 using the SHELXLTL software package. All non-hydrogen atoms were refined anisotropically and the positions of hydrogen atoms were generated geometrically. In the SHG measurements, the crystal samples were ground and filtrated with particle size at 100–150 μm. The laser beam with low divergence (pumped by an Nd:YAG laser, $\lambda = 1064$ nm, 5 ns pulse duration, 10 Hz repetition rate) was employed as fundamental beam. The instrument is model FLS 920, Edinburgh Instrument with temperature range of 10–325 K, DE 202, while laser is Vibrant 355 II, OPOTEK.

Received: January 16, 2012
Published online: March 13, 2012

Keywords: dielectric compounds · ferroelectricity · hydrogen bonds · phase transitions

[1] M. E. Lines, A. M. Glass, *Principles and Applications of Ferroelectrics and Related Materials*, Oxford University Press, New York, **1977**.

[2] a) J. Valasek, *Phys. Rev.* **1921**, *17*, 475 – 481; b) C. H. Ahn, K. M. Rabe, J.-M. Triscone, *Science* **2004**, *303*, 488 – 491; c) J. F. Scott, *Science* **2007**, *315*, 954 – 959; d) T. Hang, W. Zhang, H.-Y. Ye, R.-G. Xiong, *Chem. Soc. Rev.* **2011**, *40*, 3577 – 3598; e) R. Jakubas, Z. Ciunik, G. Bator, *Phys. Rev. B* **2003**, *67*, 024103; f) M. Szafrański, *J. Phys. Chem. B* **2011**, *115*, 8755 – 8762; g) G.-C. Xu, W. Zhang, X.-M. Ma, Y.-H. Chen, L. Zhang, H.-L. Cai, Z.-M. Wang, R.-G. Xiong, S. Gao, *J. Am. Chem. Soc.* **2011**, *133*, 14948 – 14951; h) A. Katrusiak, M. Szafrański, *Phys. Rev. Lett.* **1999**, *82*, 576 – 579; i) S. Horiuchi, Y. Tokura, *Nat. Mater.* **2008**, *7*, 357 – 366; j) S. Horiuchi, Y. Tokunaga, G. Giovannetti, S. Picozzi, H. Itoh, R. Shimano, R. Kumai, Y. Tokura, *Nature* **2010**, *463*, 789 – 792.

[3] a) H.-Y. Ye, D.-W. Fu, Y. Zhang, W. Zhang, R.-G. Xiong, S. D. Huang, *J. Am. Chem. Soc.* **2009**, *131*, 42 – 43; b) P. Tomaszewski, *Phase Transitions* **1992**, *38*, 127 – 220; c) A. Katrusiak, *Phys. Rev. B* **1993**, *48*, 2992 – 3002.

[4] a) W. Zhang, R.-G. Xiong, *Chem. Rev.* **2011**, DOI: 10.1021/cr200174w; b) D.-W. Fu, W. Zhang, H.-L. Cai, Y. Zhang, J.-Z. Ge, R.-G. Xiong, S. D. Huang, *J. Am. Chem. Soc.* **2011**, *133*, 12780 – 12786; c) H.-L. Cai, W. Zhang, J.-Z. Ge, Y. Zhang, K. Awaga, T. Nakamura, R.-G. Xiong, *Phys. Rev. Lett.* **2011**, *107*, 147601.

[5] a) B. C. Frazer, M. Mckeown, R. Pepinsky, *Phys. Rev.* **1954**, *94*, 1435; b) E. Suzuki, A. Amano, R. Nozaki, Y. Shiozaki, *Ferroelectrics* **1994**, *152*, 385 – 390; c) E. Suzuki, Y. Shiozaki, *Phys. Rev. B* **1996**, *53*, 5217 – 5221; d) Z.-W. Yin, *Dielectric Physics*, Science Press, Beijing, **2006**.

[6] a) M. Szafrański, A. Katrusiak, G. J. McIntyre, *Phys. Rev. Lett.* **2002**, *89*, 215507 – 4; b) S. Horiuchi, F. Ishii, R. Kumai, Y. Okimoto, H. Tachibana, N. Nagaosa, Y. Tokura, *Nat. Mater.* **2005**, *4*, 163 – 166; c) S. Horiuchi, R. Kumai, Y. Tokura, *Angew. Chem.* **2007**, *119*, 3567 – 3571; *Angew. Chem. Int. Ed.* **2007**, *46*, 3497 – 3501.

[7] a) G. S. Kottas, L. I. Clarke, D. Horinek, J. Michl, *Chem. Rev.* **2005**, *105*, 1281 – 1376; b) T. Akutagawa, H. Koshinaka, D. Sato, S. Takeda, S.-I. Noro, H. Takahashi, R. Kumai, Y. Tokura, T. Nakamura, *Nat. Mater.* **2009**, *8*, 342 – 347; c) W. Zhang, Y. Cai, R.-G. Xiong, H. Yoshikawa, K. Awaga, *Angew. Chem.* **2010**, *122*, 6758 – 6760; *Angew. Chem. Int. Ed.* **2010**, *49*, 6608 – 6610.

[8] Crystal data for **1** at room temperature (293 K): $C_{10}H_{14}N_4O_6$, block, $0.6 \times 0.5 \times 0.2$ mm^3, $M_r = 286.25$, Orthorhombic, $P2_12_12_1$, $a = 8.4571(6)$, $b = 10.6347(11)$, $c = 14.1341(17)$ Å, $Z = 4$, $V = 1271.2(2)$ Å^3, $\rho_{cal.} = 1.496$ g cm^{-3}, R_1 $(I > 2\sigma(I)) = 0.0682$, wR_2 (all data) $= 0.1668$, $S = 1.119$; **1** at 93 K: $C_{10}H_{14}N_4O_6$, block, $0.6 \times 0.5 \times 0.2$ mm^3, $M_r = 286.25$, Monoclinic, $P2_1$, $a = 10.578(4)$, $b = 8.389(3)$, $c = 14.093(6)$ Å, $\beta = 90.224(5)°$, $V = 1250.6(8)$ Å^3, $Z = 4$, $\rho_{cal.} = 1.520$ g cm^{-3}, R_1 $(I > 2\sigma(I)) = 0.0628$, wR_2 (all data) $= 0.2109$, $S = 0.984$. CCDC 850725 and 850726 contain the supplementary crystallographic data for this paper. These data can be obtained free of charge from The Cambridge Crystallographic Data Centre via www.ccdc.cam.ac.uk/data_request/cif.

[9] a) W. Zhang, L.-Z. Chen, R.-G. Xiong, T. Nakamura, S. D. Huang, *J. Am. Chem. Soc.* **2009**, *131*, 12544 – 12545; b) G.-C. Xu, X.-M. Ma, L. Zhang, Z.-M. Wang, S. Gao, *J. Am. Chem. Soc.* **2010**, *132*, 9588 – 9590.

[10] a) Q. Ye, Y.-M. Song, G.-X. Wang, K. Chen, D.-W. Fu, P. W. Chan, J.-S. Zhu, S. D. Huang, R.-G. Xiong, *J. Am. Chem. Soc.* **2006**, *128*, 6554 – 6555; b) X.-L. Li, K. Chen, Y. Liu, Z.-X. Wang, T. W. Wang, J.-L. Zuo, Y.-Z. Li, Y. Wang, J.-S. Zhu, J.-M. Liu, Y. Song, X.-Z. You, *Angew. Chem.* **2007**, *119*, 6944 – 6947; *Angew. Chem. Int. Ed.* **2007**, *46*, 6820 – 6823; c) G. Xu, Y. Li, W.-W. Zhou, G.-J. Wang, X.-F. Long, L.-Z. Cai, M.-S. Wang, G.-C. Guo, J.-S. Huang, G. Batorb, R. Jakubasb, *J. Mater. Chem.* **2009**, *19*, 2179 – 2183.

[11] a) F. Sandy, R. V. Jones, *Phys. Rev.* **1968**, *168*, 481 – 493; b) W. Heywang, K. Lubitz, W. Wersing, *Piezoelectricity*, Springer, **2008**, Chapter 5; c) Q. M. Zhang, V. Bharti, X. Zhao, *Science* **1998**, *280*, 2101 – 2104; d) D.-W. Fu, W. Zhang, H.-L. Cai, Y. Zhang, J.-Z. Ge, R.-G. Xiong, S. D. Huang, T. Nakamura, *Angew. Chem.* **2011**, *123*, 12153 – 12157; *Angew. Chem. Int. Ed.* **2011**, *50*, 11947 – 11951.

[12] a) M. Fiebig, T. Lottermoser, D. Fröhlich, A. V. Goltsev, R. V. Pisarev, *Nature* **2002**, *419*, 818 – 820; b) D.-W. Fu, W. Zhang, H.-L. Cai, J.-Z. Ge, Y. Zhang, R.-G. Xiong, *Adv. Mater.* **2011**, *23*, 5658 – 5662; c) J. H. Lee, L. Fang, E. Vlahos, X. Ke, Y. W. Jung, L. Fitting Kourkoutis, J.-W. Kim, P. J. Ryan, T. Heeg, M. Roeckerath, V. Goian, M. Bernhagen, R. Uecker, P. C. Hammel, K. M. Rabe, S. Kamba, J. Schubert, J. W. Freeland, D. A. Muller, C. J. Fennie, P. Schiffer, V. Gopalan, E. Johnston-Halperin, D. G. Schlom, *Nature* **2010**, *466*, 954 – 958.

[13] M. Tokunaga, *J. Phys. Soc. Jpn.* **1988**, *57*, 4275 – 4283.

[14] a) Y. Shiozaki, T. Mitsui, *Acta Crystallogr. Sect. A* **1972**, *28*, S185 – S186; b) Y. Iwata, S. Mitani, I. Shibuya, *Ferroelectrics* **1989**, *96*, 215 – 219; c) Y. Iwata, S. Mitani, I. Shibuya, *Ferroelectrics* **1990**, *107*, 287 – 292.

[15] K. Kawamura, A. Onodera, *J. Korean Phys. Soc.* **1998**, *32*, S77 – S80.

